https://doi.org/10.26565/2220-637X-2024-43-02 ISSN 2220-637X
УДК: 544.165+577.29

EVOLUTIONARY STRUCTURE OPTIMIZATION OF ENSITRELVIR AS NON-COVALENT INHIBITOR OF SARS-COV-2 MAIN PROTEASE M^{PRO}

K. O. Lohachova[a], A. S. Sviatenko[b], A. V. Kyrychenko[c], O. N. Kalugin[d]

V. N. Karazin Kharkiv National University, School of Chemistry, 4 Svobody sqr., Kharkiv, 61022 Ukraine

a) ekaterinalogatcheva@gmail.com https://orcid.org/0000-0001-7826-8320
b) anastasiia.sviatenko@student.karazin.ua https://orcid.org/0009-0007-2452-1168
c) a.v.kyrychenko@karazin.ua https://orcid.org/0000-0002-6223-0990
d) onkalugin@gmail.com https://orcid.org/0000-0003-3273-9259

Ensitrelvir is a non-covalent, non-peptide inhibitor of the SARS-CoV-2 main protease, M^{pro}. It has demonstrated effective antiviral activity against various coronavirus variants *in vitro*, along with favorable drug metabolism and pharmacokinetic profiles suitable for oral treatment. Thus, developing novel analogues of ensitrelvir is of great importance. In this study, we conducted *in silico* design of its analogues by employing evolutionary structure optimization of the parent ensitrelvir scaffold. In the first stage, we generated a virtual evolutionary library consisting of 6334 new analogues based on a series of fitness criteria, including molecular weight (M_w), cLogP, polar surface area, structural and conformational similarity, flexibility, and molecular shape. Next, we filtered the evolutionary library using a 3D pharmacophore model created from the available X-ray structure of the co-crystallized complex of ensitrelvir and M^{pro}. We then performed molecular docking calculations to rank the selected candidates according to their binding affinity and selectivity for the M^{pro} receptor. This binding score ranking allowed us to identify ten analogues of ensitrelvir that exhibit superior binding affinity to the protease M^{pro} compared to the original ensitrelvir inhibitor. Our evolutionary structure optimization indicates that the primary structural modifications that enhance the overall antiviral effect of ensitrelvir are found in the 1-methyl-1*H*-1,2,4-triazole and 6-chloro-2-methyl-2*H*-indazole fragments.

Keywords: coronavirus, COVID-19, heterocyclic compounds, M^{pro}, evolutionary library, molecular docking.

Introduction

Severe acute respiratory syndrome coronavirus 2 (SARS-CoV-2), which emerged in late 2019, led to a global epidemic and was declared a pandemic by the World Health Organization (WHO) on March 11, 2020 [1]. The 2019 coronavirus disease (COVID-19) pandemic has left an irreversible impact on the world, with more than 18 million deaths and significant disruptions to the global economy that continue to be felt today [2]. The rapid introduction of vaccines has effectively reduced the risk of severe illness from the disease [3-4]. COVID-19, caused by the highly contagious and mutating SARS-CoV-2, saw the Omicron variant replace the Delta variant, and it continues to evolve into various new strains. This ongoing evolution presents substantial challenges for healthcare systems and public health infrastructure [5-7]. Overall statistics indicate that vaccination does not provide long-lasting immunity against the SARS-CoV-2 virus. Although the outbreak of COVID-19 has transitioned to a more normalized phase, ongoing research into inhibitors remains crucial for the prevention of future coronavirus pandemics [8-9].

COVID-19 is a respiratory disease caused by the SARS-CoV-2 virus, which is a positive single-stranded RNA virus [10]. This virus contains several structural proteins, including the nucleocapsid protein (N), spike protein (S), envelope protein (E), and membrane glycoprotein (M), along with its RNA genome. SARS-CoV-2 is classified as part of the β-coronavirus genus, which also includes SARS-CoV, HCoV-OC43, HCoV-HKU1, and MERS-CoV.

Structural proteins, particularly spike (S) proteins, are crucial in viral pathogenesis as they facilitate receptor recognition and membrane fusion. Although E proteins are the smallest structural proteins, they are essential for viral assembly, budding, envelope formation, and overall pathogenicity. M proteins play a key role in the assembly of the virus, while N proteins have multiple functions, including the packaging of the viral RNA genome. Nonstructural proteins of SARS-CoV-2, such as the main protease (M^{pro}) and RNA-dependent RNA polymerase (RdRp), are highly conserved across different virus strains. This conservation makes them attractive targets for drug development, as targeting these

© Lohachova K. O., Sviatenko A. S., Kyrychenko A. V., Kalugin O. N., 2024
This is an open access article distributed under the terms of the Creative Commons Attribution License 4.0.

proteins can minimize interference with host cell physiological processes [11-13]. Importantly, the major protease (M^{pro}) of SARS-CoV-2 exhibits unique substrate specificity by cleaving peptides exclusively after glutamine residues, which reduces the risk of host cell toxicity from inhibitors targeting M^{pro}. Inhibition of SARS-CoV-2 M^{pro} has become a promising approach for the development of therapeutics for the treatment of COVID-19 [1, 14] (Fig. 1). M^{pro} is characterized as a three-domain cysteine protease with a catalytic dyad consisting of Cys145–His41 located in the cleft between Domains I and II [1, 15].

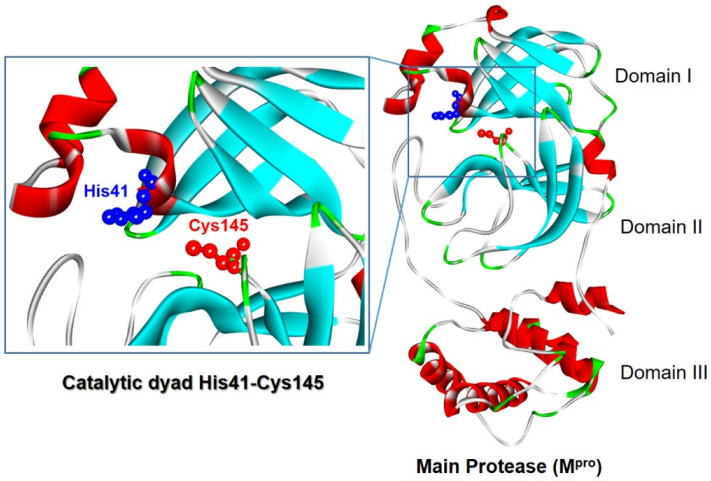

Figure 1. The X-ray structure and a binding site of the main cysteine protease M^{pro} of SARS-CoV-2 (PDB: 8HEF) [16]. An insert shows the M^{pro} binding site and two crucial catalytic residues of His41 and Cys145, are rendered as *blue* and *red* sticks, respectively.

Shionogi Pharmaceutical Company, in collaboration with Hokkaido University, has developed a non-peptide oral drug called ensitrelvir (experimental name S-217622, systematic name 1-(2,4,5-trifluorobenzyl)-3-[(1-methyl-1H-1,2,4-triazol-3-yl)methyl]-(6E)-6-[(6-chloro-2-methyl-2H-indazol-5-yl)-imino]-1,3,5-triazinane-2,4-dione, see Fig. 2a). This drug received approval for sale in Japan on November 22, 2022 [17]. The molecule was discovered through a process that included virtual screening, biological analysis, and optimization of the hit compound using a structure-based drug design approach. The X-ray crystal structure of the ensitrelvir complex with the M^{pro} enzyme reveals that the 1-methyl-1H-1,2,4-triazole link at the S1 position forms a H-bond of 2.99 Å with the side chain NH of H163 (see Fig. 2b) .

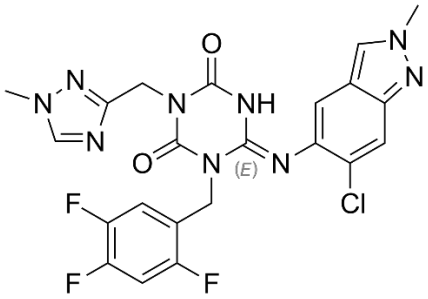

Ensitrelvir (S-217622)

(a)

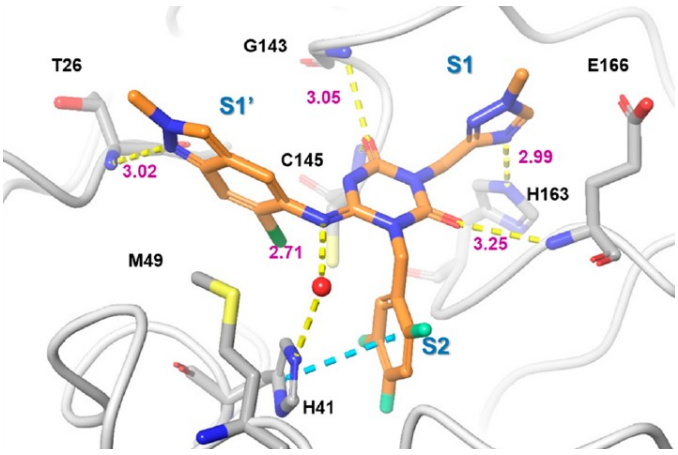

(b)

Figure 2. (a) Chemical structure of ensitrelvir. (b) The X-ray crystal structure of the ensitrelvir complex with M^{pro} (PDB: 8HEF). Adapted with permission by [16]. Copyright © 2022. The Authors. Published by American Chemical Society.

In addition, the trifluorobenzyl group of ensitrelvir occupies the S2 hydrophobic pocket, aligning parallel to the histidine H41 ring, which enhances contact. The 6-chloro-2-methyl-2H-indazole fragment, located in the S1' pocket, forms a H-bond of 3.02 Å with the NH of the main chain at T26 and maintains hydrophobic interactions with M49. Finally, one of the carbonyl groups of the 1,3,5-triazinane-2,4-dione moiety forms a H-bond of 3.25 Å with the NH of E166.

Ensitrelvir showed significant inhibitory activity against SARS-CoV-2 M^{pro} as a non-covalent non-peptide inhibitor, with an IC_{50} value of 0.013 μM and the effective antiviral activity with an EC_{50} value of 0.37 μM [17, 18]. It has demonstrated antiviral activity against a number of SARS-CoV-2 variants and coronaviruses *in vitro*, as well as favorable drug metabolism and pharmacokinetic profiles for oral dosing [21-24].

Therefore, the purpose of this research is to investigate the non-covalent interactions between ligands and proteins. This study will focus on a virtual evolutionary library created based on the drug ensitrelvir and a leading compound that exhibits better affinity for the main M^{pro} protease of the SARS-CoV-2 virus.

Evolutionary Algorithm

To generate the evolutionary library of ensitrelvir analogues we used OSIRIS DataWarrior software [25]. The evolutionary algorithm mimics natural evolution and starts with a small initial set of molecules (first parent derivative) [26]. In the next step, several derivatives, new but similar molecules, are created by applying a small random structural modification (the first progeny generation). Modifications such as single atom replacement, atom insertion, bond reordering, substituent migration, ring aromatization, chiral center inversion, etc. are applied (Fig. 3). Each modification is then evaluated on how well it meets the target criteria.

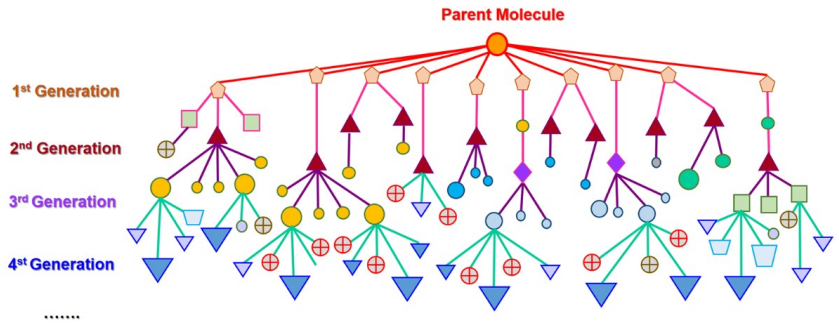

Figure 3. General scheme for generating the Evolutionary Library Tree. Bigger size symbols represent the 1st, 2nd, 3rd, and 4th survived generations, while smaller symbols illustrate some unsuccessful branches that did not evolve into the next generation.

In a next step, the algorithm applies customizable fitness criteria to rank the new generation's molecules according to these criteria. The highest ranking molecules from this generation are selected to survive and form the parent molecules for the next generation. Typically, after about one or a few hundred molecule generations DataWarrior has arrived at structures that optimally match the defined fitness criteria..

Molecular docking setup

Molecular docking was carried out for all the synthesized compounds against the main protease M^{pro} (PDB: 8HEF) of SARS-CoV-2 [17]. The preparation of the receptor and ligands were carried out with the LigandScout software, version 4.5 [27]. Molecular docking calculations were performed with the built-in version of the AutoDock Vina 1.1.2 software [28]. We carried out the semi-flexible docking, so that the receptor was kept rigid and the ligand molecules were conformational flexible. In the Autodock Vina, the Lamarckian genetic algorithm was used as a research parameter. For each ligand, three independent runs were performed using different random seeds. The best docking mode corresponds to the largest ligand-binding affinity. Molecular graphics and visualization were performed using VMD 1.9.3 [23].

Results and Discussion

Generation of Evolutionary Library of *Ensitrelvir Analogues*

To create a library of new molecules that are structurally similar to the original structure of ensitrelvir, several approaches can be employed [30]. One promising method involves generating a virtual library of ensitrelvir analogs using DataWarrior software [25]. This process utilizes an evolutionary algorithm that mimics the natural evolution of drug-like substances. The creation of new molecules follows a specific procedure: it begins with the ensitrelvir molecule (Fig. 2a), referred to as the "first generation" (Fig. 3). From this starting point, a series of similar derivatives are generated by applying minor random structural modifications to the parent structure. Each new modification is then assessed based on its adherence to nine selected suitability criteria, including molecular weight (M_w), logarithm of the partition coefficient (cLogP), polar surface area (PSA) [31], molecular shape, flexibility, and others (Table 1). The selection principles for these fitness criteria are discussed in more details in our recent works [26, 32].

Table 1. Selected fitness criteria and their parameters used to create a virtual evolutionary library of ensitrelvir analogues.

Fitness criteria	Settings
Number of generations	25
Compounds per generation	2048
Compounds survive a generation	256
Structure similarity	algorithm OrgFunctions target - ensitrelvir
Conformational similarity	algorithm PheSA
Molecular weight (M_w)	400-500 g/mol
cLogP	2-4
Polar surface area	80-120 Å^2
Molecular flexibility	0.3-0.7
Molecular shape	0.3-0.7
H-donors	3-5
H-acceptors	5-10
Rotatable bond count	4-8

Structural mutations that meet these criteria are more likely to occur. In the current generation, the new counterparts were organized according to these criteria, allowing the molecules with the highest ranking to be selected for survival and to serve as parent molecules for the next generation. Following this evolutionary algorithm, a total of 25 generations were produced, resulting in 6334 virtual ensitrelvir analogs.

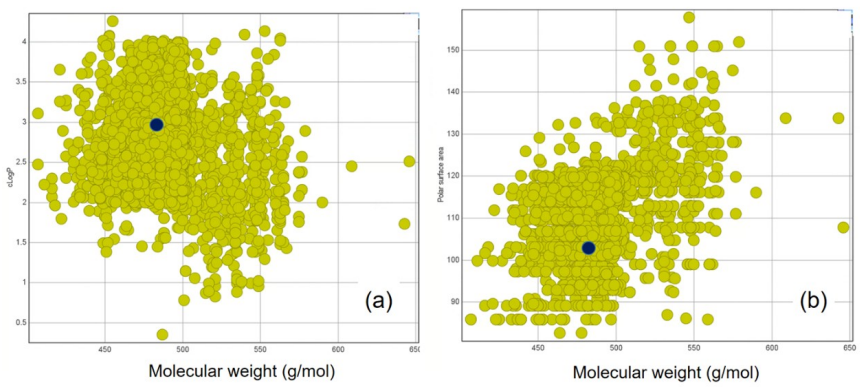

Figure 4. Two-dimensional graph of molecular weight distribution versus cLogP (a) and PSA (b) parameters for the created evolutionary library. The blue points indicate the parent ensitrelvir molecule.

The evolutionary library of ensitrelvir derivatives was generated based on the principle of structural variation, as well as by applying specific fitness criteria (see Table 1). These criteria included molecular weight (400 g/mol < M_w < 500 g/mol), polar surface area (80 Å² < PSA < 120 Å²), and cLogP values (2 < cLogP < 4). Figure 4 illustrates the two-dimensional distribution of these parameters within the generated library, which exhibits a symmetric distribution.

3D Pharmacophore Screening

The created evolutionary library is large enough to verify its direction by the method of molecular docking. Therefore, at first the library was further analyzed and filtered *in silico* according to the criterion of the correspondence of each new molecule to the 3D model of the ensitrelvir pharmacophore [33]. The pharmacophore model was created using the LigandScout software package [27] (Fig. 5) based on the first available crystal structure of ensitrelvir in complex with M^{pro} (PDB: 8HEF) [16]. The screening procedure relative to the ensitrelvir 3D-pharmacophore model made it possible to reduce the chemical space of the library from 6334 virtual molecules to 41 active ensitrelvir derivatives that have pharmacophore structural similarity to the initial structure. In this pharmacophore filtering, a pharmacophore-fit score cut-off of 75 or higher was utilized.

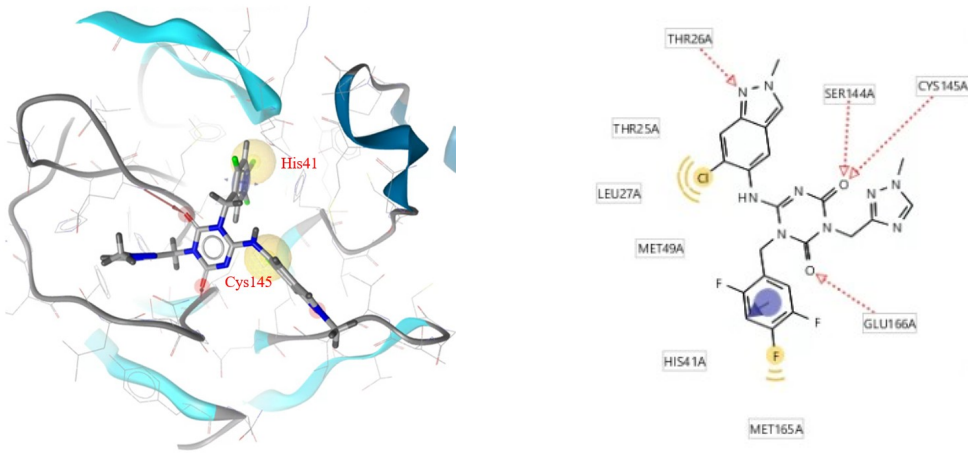

(a) (b)

Figure 5. (a) 3D model of the ensitrelvir pharmacophore constructed from its crystal structure in complex with M^{pro} (PDB: 8HEF) [16]. The labeled His41 and Cys145 residues are the active site of M^{pro}. (b) Scheme of intermolecular interactions of ensitrelvir with key surrounding residues of M^{pro}.

Molecular Docking of Evolutionary Library

To identify potential leader compounds from the evolutionary library, we evaluated the binding affinities of 41 selected active candidates by performing molecular docking with M^{pro} using LigandScout software [27]. LigandScout incorporates a built-in version of the widely used AutoDock Vina molecular docking method. To calibrate and validate the ligand-protease docking algorithm, we conducted a docking study of ensitrelvir and compared its geometry to the corresponding X-ray structural data.

Molecular docking was conducted for the selected inhibitors of the M^{pro} main protease of the SARS-CoV-2 coronavirus. The spatial structure of the main protease M^{pro} (PDB ID: 8HEF) was obtained from the Brookhaven Protein Data Bank (Fig. 6a-b) [16]. The results of the molecular docking for ensitrelvir, along with the experimental crystallographic data of its complex with Mpro, are in good agreement (Fig. 6c). This consistency allows us to use this method for the quantitative analysis of the affinity of new derivatives of ensitrelvir to M^{pro}.

The molecular docking results for the selected 41 active derivatives revealed that 10 analogues demonstrated a higher binding affinity to M^{pro} than the parent ensitrelvir. Figure 7 illustrates the struc-

tures of the top five leading ligands, along with their energetic characteristics related to the protease-ligand interaction.

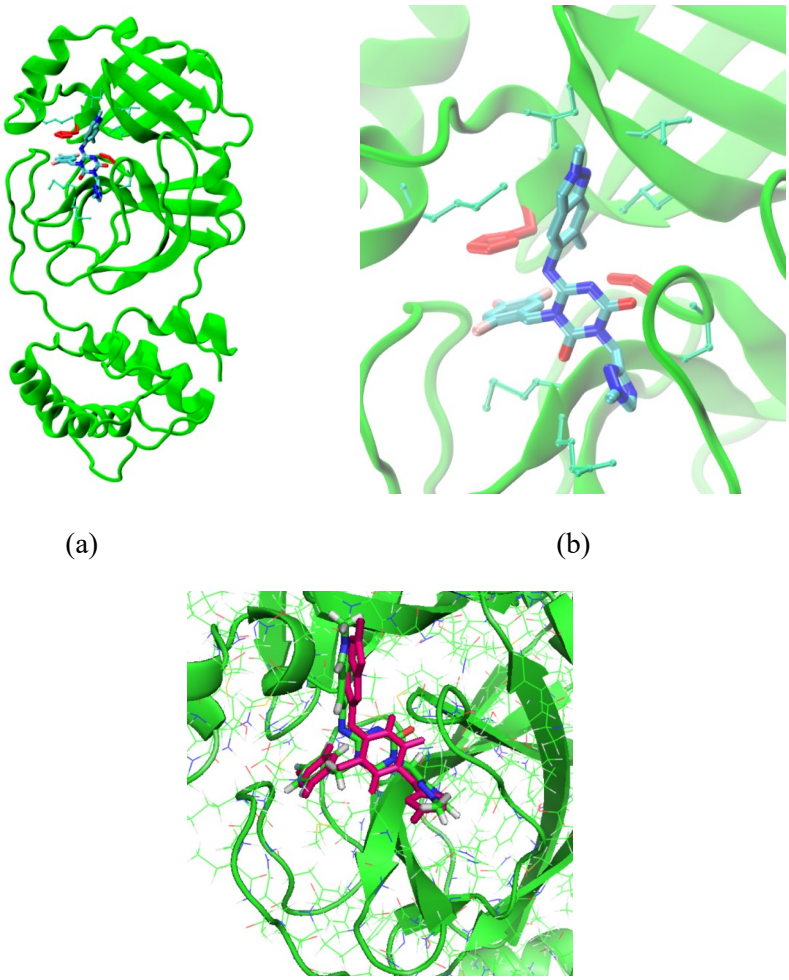

Figure 6. (a, b) Configuration of ensitrelvir incorporation into the active site of M^{pro} protease of SARS-CoV-2 virus (PDB: 8HEF) [16]. The catalytic amino acid residues His41 and Cys145 are shown in red. (c) Comparison of the molecular docking results of ensitrelvir with its crystallographic structure in complex with M^{pro}. The ligand configuration estimated by molecular docking is shown in pink.

The following parameters were considered as binding energy criteria:

1. Binding affinity as determined by the AutoDock Vina docking algorithm.
2. Binding Affinity Score (BAS) calculated using the LigandScout software package.

The BAS score accounts for both the protein-ligand binding enthalpy and the solvent effects. It is regarded as the most representative indicator and was therefore chosen for the selection of lead ligands.

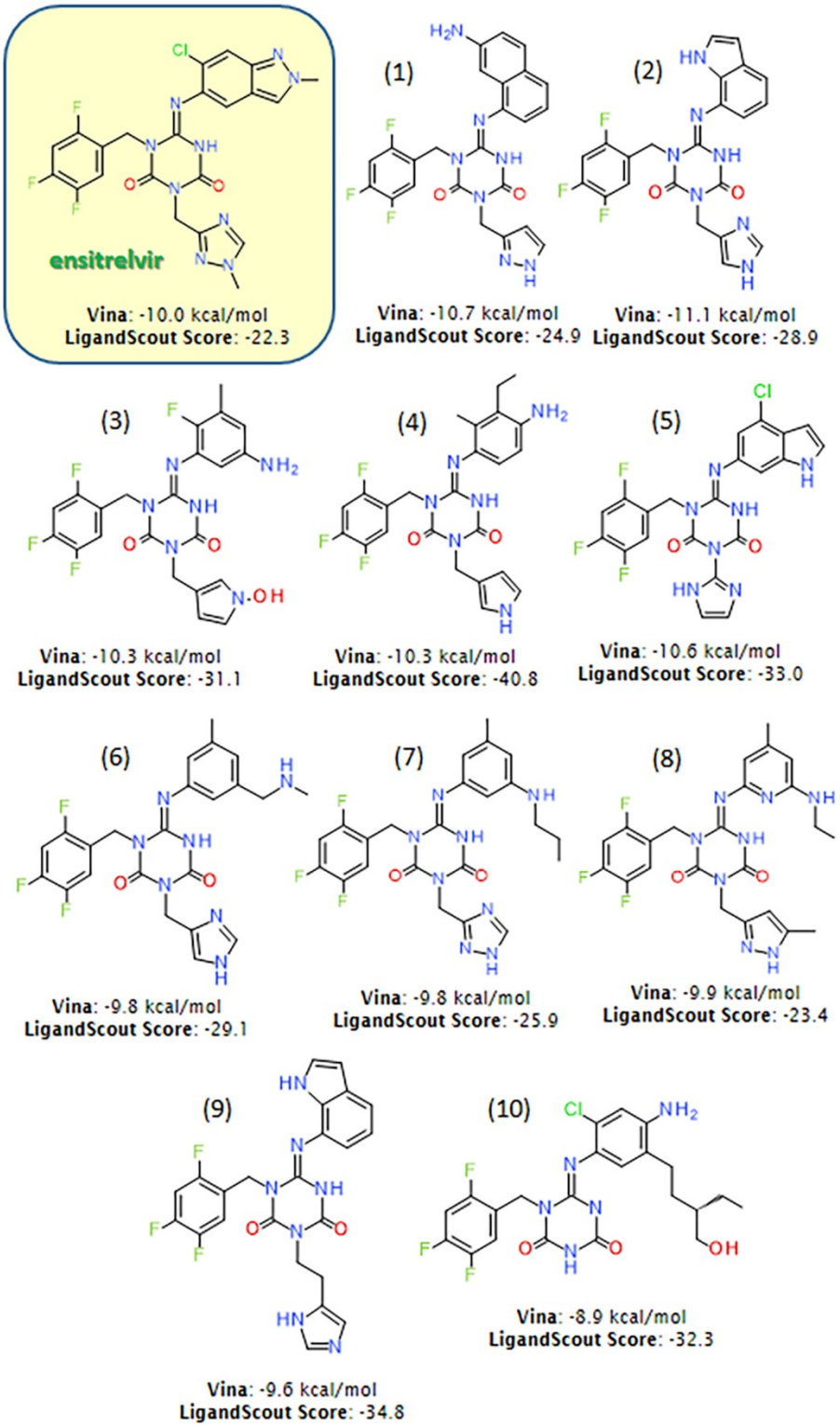

Figure 7. Molecular structure of ensitrelvir and its analogues (**1-10**), which show the higher binding affinity to M^{pro} compared to the parent ensitrelvir.

A key structural feature of the binding and docking of the selected inhibitors with the active site of M^{pro} is the maintenance of the configuration of the trifluorobenzyl fragment, as seen in derivatives **1-10** illustrated in Figures 7 and 8, respectively. Efforts to replace the 2,4,5-trifluorobenzyl moiety of ensitrelvir did not enhance the binding affinity. The overall binding affinity of these inhibitors

increases due to structural modifications in other parts of the molecule. The primary structural modifications observed in inhibitors **1-10** occur in two specific fragments of the ensitrelvir molecule: the 1-methyl-1H-1,2,4-triazole and the 6-chloro-2-methyl-2H-indazole fragments (see Fig. 7).

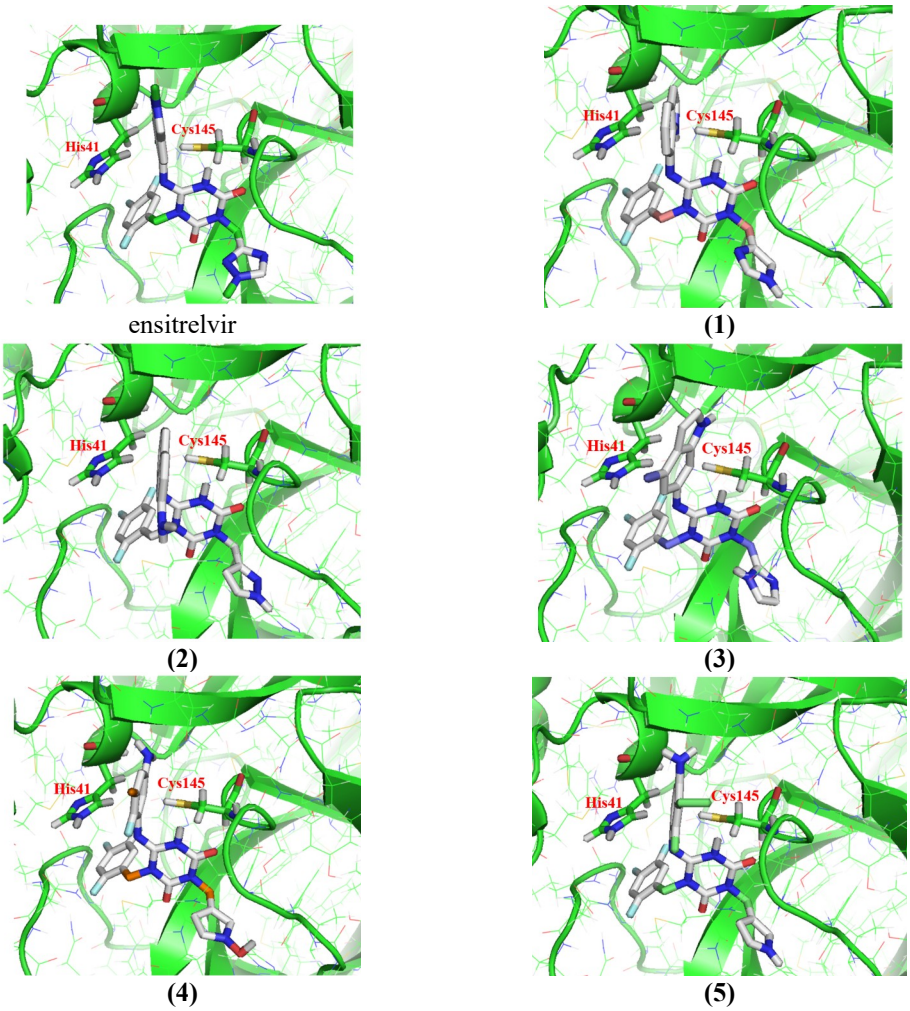

Figure 8. The best binding modes of ensitrelvir and its analogues **1-5** with the active center of M_{pro} protease of the SARS-CoV-2 virus (PDB: 8HEF).

The results presented in Figures 7 and 8 indicate that the increase in the binding energy and the enhancement of the overall affinity score result from paired structural modifications of the initial structure of ensitrelvir (1). These changes include: replacing the methyl-1,2,4-triazole and 6-chloro-2-methyl-2H-indazole with a pyrazole ring and aminonaphthol (ligand **1**), an imidazole ring and an indole ring (ligand **2**), chlorindole and an imidazole ring (ligand **5**), fluoromethylaniline and a hydroxypyrrole ring (ligand **3**), and ethylmethylaniline and a pyrrole ring (ligand **4**). These modifications significantly contribute to enhancing the antiviral efficacy of the ensitrelvir derivatives.

Conclusions

Modern methods for discovering new potential drugs increasingly rely on computer modeling techniques [14, 26, 30, 34-36]. In this study, design of novel analogues of ensitrelvir was conducted by employing evolutionary structure optimization of the parent ensitrelvir scaffold as summarized in Fig. 9.

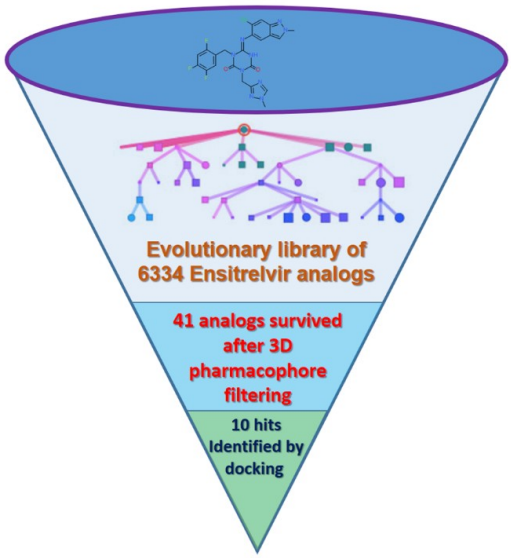

Figure 9. Workflow of discovery of novel ensitrelvir analogs

A library of 6,334 structurally similar ensitrelvir derivatives was created using a set of fitness criteria, including molecular weight (M_w), cLogP, polar surface area, structural and conformational similarity, flexibility, and molecular shape. Further filtering of this library based on its correspondence to a 3D pharmacophore model of ensitrelvir led to the identification of 41 promising derivatives. Subsequently, a detailed structural and energetic analysis of the binding affinity of these candidate derivatives to the M^{pro} protease was conducted using molecular docking methods. This analysis allowed us to select 10 ensitrelvir analogues that exhibit a stronger binding affinity to the M^{pro} protease compared to the original ensitrelvir inhibitor. Finally, we demonstrated for the first time that the key structural modifications responsible for enhancing the overall antiviral effectiveness of the inhibitor are found in the 1-methyl-1H-1,2,4-triazole and 6-chloro-2-methyl-2H-indazole fragments of ensitrelvir. We believe that our proposed workflow for evolutionary optimization of existing scaffolds of approved drugs is a promising, cost-effective strategy for developing new antiviral agents against COVID-19 [37].

Acknowledgement

The authors acknowledge the grant 2021.01/0062 "*Molecular design, synthesis and screening of new potential antiviral pharmaceutical ingredients for the treatment of infectious diseases COVID-19*" from the National Research Foundation of Ukraine.

The authors thank Prof. T. Langer from University of Vienna for giving us the opportunity to use LigandScout 4.4.9 suite.

References

1. Yevsieieva L. V., Lohachova K. O., Kyrychenko A., Kovalenko S. M., Ivanov V. V., Kalugin O. N. Main and papain-like proteases as prospective targets for pharmacological treatment of coronavirus SARS-CoV-2. *RSC Adv.* **2023**, *13* (50), 35500–35524. https://doi.org/10.1039/d3ra06479d
2. Polatoğlu I., Oncu-Oner T., Dalman I., Ozdogan S. COVID-19 in early 2023: Structure, replication mechanism, variants of SARS-CoV-2, diagnostic tests, and vaccine & drug development studies. *MedComm* **2023**, *4* (2), e228. https://doi.org/10.1002/mco2.228
3. Lau J. J., Cheng S. M. S., Leung K., Lee C. K., Hachim A., Tsang L. C. H., Yam K. W. H., Chaothai S., Kwan K. K. H., Chai Z. Y. H., Lo T. H. K., Mori M., Wu C., Valkenburg S. A., Amarasinghe G. K., Lau E. H. Y., Hui D. S. C., Leung G. M., Peiris M., Wu J. T. Real-world COVID-19 vaccine effectiveness against the Omicron Ba.2 variant in a SARS-CoV-2 infection-naive population. *Nat. Med.* **2023**, *29* (2), 348-357. https://doi.org/10.1038/s41591-023-02219-5
4. Fischer C., Willscher E., Paschold L., Gottschick C., Klee B., Diexer S., Bosurgi L., Dutzmann J., Sedding D., Frese T., Girndt M., Hoell J. I., Gekle M., Addo M. M., Schulze zur Wiesch J.,

Mikolajczyk R., Binder M., Schultheiß C. SARS-CoV-2 vaccination may mitigate dysregulation of IL-1/IL-18 and gastrointestinal symptoms of the post-COVID-19 condition. *npj Vaccines* **2024**, *9* (1), 23. https://doi.org/10.1038/s41541-024-00815-1

5. Carabelli A. M., Peacock T. P., Thorne L. G., Harvey W. T., Hughes J., de Silva T. I., Peacock S. J., Barclay W. S., de Silva T. I., Towers G. J., Robertson D. L., Consortium C.-G. U. SARS-CoV-2 variant biology: Immune escape, transmission and fitness. *Nat. Rev. Microbiol.* **2023**, *21* (3), 162-177. https://doi.org/10.1038/s41579-022-00841-7
6. Markov P. V., Ghafari M., Beer M., Lythgoe K., Simmonds P., Stilianakis N. I., Katzourakis A. The evolution of SARS-CoV-2. *Nat. Rev. Microbiol.* **2023**, *21* (6), 361-379. https://doi.org/10.1038/s41579-023-00878-2
7. Uriu K., Ito J., Zahradnik J., Fujita S., Kosugi Y., Schreiber G., Sato K. Enhanced transmissibility, infectivity, and immune resistance of the SARS-CoV-2 omicron Xbb.1.5 variant. *Lancet. Infect. Dis.* **2023**, *23* (3), 280-281. https://doi.org/10.1016/S1473-3099(23)00051-8
8. Wang Z., Yang L. Post-acute sequelae of SARS-CoV-2 infection: A neglected public health issue. *Front. Public Health* **2022**, *10,* 908757. https://doi.org/10.3389/fpubh.2022.908757
9. Davis H. E., McCorkell L., Vogel J. M., Topol E. J. Long COVID: Major findings, mechanisms and recommendations. *Nat. Rev. Microbiol.* **2023**, *21* (3), 133-146. https://doi.org/10.1038/s41579-022-00846-2
10. Blomberg B., Mohn K. G.-I., Brokstad K. A., Zhou F., Linchausen D. W., Hansen B.-A., Lartey S., Onyango T. B., Kuwelker K., Sævik M., Bartsch H., Tøndel C., Kittang B. R., Madsen A., Bredholt G., Vahokoski J., Fjelltveit E. B., Bansal A., Trieu M. C., Ljostveit S., Olofsson J. S., Ertesvåg N., Sandnes H. H., Corydon A., Søyland H., Eidsheim M., Jakobsen K., Guldseth N., Hauge S., Cox R. J., Langeland N., Bergen C.-R. G. Long COVID in a prospective cohort of home-isolated patients. *Nat. Med.* **2021**, *27* (9), 1607-1613. https://doi.org/10.1038/s41591-021-01433-3
11. Walker A. P., Fan H., Keown J. R., Knight M. L., Grimes Jonathan M., Fodor E. The SARS-CoV-2 RNA polymerase is a viral rna capping enzyme. *Nucleic Acids Res.* **2021**, *49* (22), 13019-13030. https://doi.org/ 10.1093/nar/gkab1160
12. Yin W., Mao C., Luan X., Shen D.-D., Shen Q., Su H., Wang X., Zhou F., Zhao W., Gao M., Chang S., Xie Y.-C., Tian G., Jiang H.-W., Tao S.-C., Shen J., Jiang Y., Jiang H., Xu Y., Zhang S., Zhang Y., Xu H. E. Structural basis for inhibition of the RNA-dependent RNA polymerase from SARS-CoV-2 by Remdesivir. *Science* **2020**, *368* (6498), 1499. https://doi.org/10.1126/science.abc1560
13. Poduri R., Joshi G., Jagadeesh G. Drugs targeting various stages of the SARS-CoV-2 life cycle: Exploring promising drugs for the treatment of COVID-19. *Cellular Signalling* **2020**, *74* 109721. https://doi.org/10.1016/j.cellsig.2020.109721
14. Zakharov A. B., Kyrpa M., Kyrychenko A. V., Kovalenko S. M., Kalugin O. N., Ivanov V. V., Adamowicz L. Towards the computational design of organic molecules with specified properties. *Struct. Chem.* **2025**, *36* (2), 723-738. https://doi.org/10.1007/s11224-024-02441-y
15. ., Lagarias P., Gao A., Townsend J. A., Meng X., Dube P., Zhang X., Hu Y., Kitamura N., Hurst B., Tarbet B., Marty M. T., Kolocouris A., Xiang Y., Chen Y., Wang J. Structure and inhibition of the SARS-CoV-2 main protease reveal strategy for developing dual inhibitors against Mpro and Cathepsin l. *Sci. Adv.* **2020**, *6* (50), eabe0751. https://doi.org/10.1126/sciadv.abe0751
17. Unoh Y., Uehara S., Nakahara K., Nobori H., Yamatsu Y., Yamamoto S., Maruyama Y., Taoda Y., Kasamatsu K., Suto T., Kouki K., Nakahashi A., Kawashima S., Sanaki T., Toba S., Uemura K., Mizutare T., Ando S., Sasaki M., Orba Y., Sawa H., Sato A., Sato T., Kato T., Tachibana Y. Discovery of S-217622, a noncovalent oral SARS-CoV-2 3CL protease inhibitor clinical candidate for treating COVID-19. *J. Med. Chem.* **2022**, *65* (9), 6499-6512. https://doi.org/10.1021/ acs.jmedchem.2c00117
18. Noske G. D., de Souza Silva E., de Godoy M. O., Dolci I., Fernandes R. S., Guido R. V. C., Sjö P., Oliva G., Godoy A. S. Structural basis of Nirmatrelvir and Ensitrelvir activity against naturally occurring polymorphisms of the SARS-CoV-2 main protease. *J. Biol. Chem.* **2023**, *299* (3). https://doi.org/10.1016/j.jbc.2023.103004
19. Duan Y., Zhou H., Liu X., Iketani S., Lin M., Zhang X., Bian Q., Wang H., Sun H., Hong S. J., Culbertson B., Mohri H., Luck M. I., Zhu Y., Liu X., Lu Y., Yang X., Yang K., Sabo Y., Chavez

A., Goff S. P., Rao Z., Ho D. D., Yang H. Molecular mechanisms of SARS-CoV-2 resistance to Nirmatrelvir. *Nature* **2023**, *622* (7982), 376-382. https://doi.org/10.1038/s41586-023-06609-0

20. Kovalevsky A., Aniana A., Ghirlando R., Coates L., Drago V. N., Wear L., Gerlits O., Nashed N. T., Louis J. M. Effects of SARS-CoV-2 main protease mutations at positions L50, E166, and L167 rendering resistance to covalent and noncovalent inhibitors. *J. Med. Chem.* **2024**, *67* (20), 18478-18490. https://doi.org/10.1021/acs.jmedchem.4c01781
21. Lopez U. M., Hasan M. M., Havranek B., Islam S. M. SARS-CoV-2 resistance to small molecule inhibitors. *Curr. Clin. Micro Rpt.* **2024**, *11* (3), 127-139. https://doi.org/10.1007/s40588-024-00229-6
22. Krismer L., Schöppe H., Rauch S., Bante D., Sprenger B., Naschberger A., Costacurta F., Fürst A., Sauerwein A., Rupp B., Kaserer T., von Laer D., Heilmann E. Study of key residues in MERS-CoV and SARS-CoV-2 main proteases for resistance against clinically applied inhibitors nirmatrelvir and ensitrelvir. *npj Viruses* **2024**, *2* (1), 23. https://doi.org/10.1038/s44298-024-00028-2
23. Lin C., Jiang H., Li W., Zeng P., Zhou X., Zhang J., Li J. Structural basis for the inhibition of coronaviral main proteases by Ensitrelvir. *Structure* **2023**, *31* (9), 1016-1024.e3. https://doi.org/10.1016/j.str.2023.06.010
24. Kiso M., Yamayoshi S., Iida S., Furusawa Y., Hirata Y., Uraki R., Imai M., Suzuki T., Kawaoka Y. *In vitro* and *in vivo* characterization of SARS-CoV-2 resistance to Ensitrelvir. *Nat. Commun.* **2023**, *14* (1), 4231. https://doi.org/10.1038/s41467-023-40018-1
25. Sander T., Freyss J., von Korff M., Rufener C. Datawarrior: An open-source program for chemistry aware data visualization and analysis. *J. Chem. Inf. Model.* **2015**, *55* (2), 460-473. https://doi.org/10.1021/ci500588j
26. Lohachova K. O., Sviatenko A. S., Kyrychenko A., Ivanov V. V., Langer T., Kovalenko S. M., Kalugin O. N. Computer-aided drug design of novel nirmatrelvir analogs inhibiting main protease of coronavirus SARS-COV-2. *J. Appl. Pharm. Sci.* **2024**, *14* (5), 232-239. https://doi.org/10.7324/JAPS.2024.158114
27. Wolber G., Langer T. LigandScout: 3-D pharmacophores derived from protein-bound ligands and their use as virtual screening filters. *J. Chem. Inf. Model.* **2005**, *45* (1), 160-169. https://doi.org/10.1021/ci049885e
28. Trott O., Olson A. J. AutoDock Vina: Improving the speed and accuracy of docking with a new scoring function, efficient optimization, and multithreading. *J. Comput. Chem.* **2010**, *31* (2), 455-461. doi: https://doi.org/10.1002/jcc.21334
29. Humphrey W., Dalke A., Schulten K. VMD: Visual molecular dynamics. *J. Mol. Graphics* **1996**, *14* (1), 33-38. https://doi.org/10.1016/0263-7855(96)00018-5
30. Ivanov V., Lohachova K., Kolesnik Y., Zakharov A., Yevsieieva L., Kyrychenko A., Langer T., Kovalenko S. M., Kalugin O. M. Recent advances in computational drug discovery for therapy against coronavirus SARS-CoV-2. *ScienceRise: Pharm. Sci.* **2023**, 6(46), 4-24. https://doi.org/10.15587/2519-4852.2023.290318
31. Ertl P., Rohde B., Selzer P. Fast calculation of molecular polar surface area as a sum of fragment-based contributions and its application to the prediction of drug transport properties. *J. Med. Chem.* **2000**, *43* (20), 3714-3717. https://doi.org/10.1021/jm000942e
32. Yevsieieva L., Trostianko P., Kyrychenko A., Ivanov V., Kovalenko S., Kalugin O. Design of non-covalent dual-acting inhibitors for proteases M^{pro} and PL^{pro} of coronavirus SARS-CoV-2 through evolutionary library generation, pharmacophore profile matching, and molecular docking calculations. *Sci. Rise. Pharm. Sci.* **2024**, 6(52), 15-26. https://doi.org/10.15587/2519-4852.2024.313808
33. Ruiz-Moreno A. J., Cedillo-González R., Cordova-Bahena L., An Z., Medina-Franco J. L., Velasco-Velázquez M. A. Consensus pharmacophore strategy for identifying novel SARS-CoV-2 Mpro inhibitors from large chemical libraries. *J. Chem. Inf. Model.* **2024**, *64* (6), 1984-1995. https://doi.org/10.1021/acs.jcim.3c01439
34. Anokhin D., Kovalenko S., Trostianko P., Kyrychenko A., Zakharov A., Zubatiuk T., Ivanov V., Kalugin O. Towards the discovery of molecules with anti-COVID-19 activity: Relationships between screening and docking results. *Kharkiv University Bulletin. Chemical Series* **2024**, (42), 6-14. https://doi.org/10.26565/2220-637X-2024-42-01

35. Kyrychenko A., Bylov I., Geleverya A., Kovalenko S., Zhuravel I., Fetyukhin V., Langer T. Computer-aided rational design and synthesis of new potential antihypertensive agents among 1,2,3-triazole-containing nifedipine analogs. *SciRise: Pharm. Sci.* **2024**, *49* (3), 4-12. https://doi.org/10.15587/2519-4852.2024.291626
36. Zahrychuk H. Y., Gladkov E. S., Kyrychenko A. V., Poliovyi D. O., Zahrychuk O. M., Kucher T. V., Logoyda L. S. Structure-based rational design and virtual screening of valsartan drug analogs towards developing novel inhibitors of angiotensin II type 1 receptor. *Biointerface Res. Appl. Chem.* **2023**, *13* (5), 440. https://doi.org/10.33263/BRIAC135.440
37. Vincenzi M., Mercurio A. F., Leone M. Looking for SARS-CoV-2 therapeutics through computational approaches. *Curr. Med. Chem.* **2023**, *30* (28), 3158-3214. http://dx.doi.org/10.2174/0929867329666221004104430

Received 27.09.2024 *Accepted 19.12.2024*

К.О. Логачова, А. С. Святенко, О. В. Кириченко, О. М. Калугін. Еволюційна оптимізація будови енсітрелвіру як нековалентного інгібітора основної протеази SARS-COV-2 M^{pro}.

Харківський національний університет імені В.Н. Каразіна, хімічний факультет, майдан Свободи, 4, Харків, 61022, Україна

Енсітрелвір є нековалентним непептидним інгібітором основної протеази M^{pro} вірусу SARS-CoV-2. Він продемонстрував ефективну противірусну дію проти різних варіантів коронавірусу *in vitro*, а також сприятливий метаболізм і фармакокінетичні профілі, придатні для перорального лікування. Таким чином, розробка нових аналогів енситрелвіру має велике значення. У цьому дослідженні ми провели *in silico* дизайн його аналогів, використовуючи еволюційну оптимізацію структури батьківського скелета енсітрелвіру. На першому етапі ми створили віртуальну еволюційну бібліотеку, що складається з 6334 нових аналогів на основі ряду критеріїв придатності, включаючи молекулярну масу (M_w), cLogP, площу полярної поверхні, структурну та конформаційну подібність, гнучкість і молекулярну форму. Далі ми відфільтрували еволюційну бібліотеку за допомогою 3D-моделі фармакофора, створеної з доступної рентгенівської структури спільно кристалізованого комплексу енсітрелвіру та M^{pro}. Потім ми виконали розрахунки молекулярного докінгу, щоб класифікувати обраних кандидатів відповідно до їх афінності зв'язування та селективності до рецептора M^{pro}. Цей рейтинг зв'язування дозволив нам ідентифікувати десять аналогів енсітрелвіру, які виявляють кращу афінність зв'язування з протеазою M^{pro} порівняно з вихідним інгібітором енсітрелвіром. Наша еволюційна оптимізація структури вказує на те, що первинні структурні модифікації, які посилюють загальний противірусний ефект енсітрелвіру, розташовані у структурних фрагментах 1-метил-1H-1,2,4-тріазолу та 6-хлор-2-метил-2H-індазолу.

Ключові слова: *коронавірус, КОВІД-19, гетероциклічні сполуки, M^{pro}, еволюційна бібліотека, молекулярний докінг*

Надіслано до редакції 27.09.2024 *Прийнято до друку 19.12.2024*